

Cubic boron nitride: an experimental and theoretical ELNES study

D.N. Jayawardane, Chris J. Pickard, L.M. Brown, M.C. Payne

Cavendish Laboratory, University of Cambridge, Madingley road, Cambridge CB3 0HE, UK.

(November 3, 2018)

Abstract

A comparison between experimental and theoretical electron Energy Loss Near Edge Structure (ELNES) of B and N K-edges in cubic boron nitride is presented. The electron energy loss spectra of cubic boron nitride particles were measured using a scanning transmission electron microscope. The theoretical calculation of the ELNES was performed within the framework of density functional theory including single particle core-hole effects. It is found that experimental and calculated ELNES of both the B and N K-edges in cubic boron nitride show excellent agreement.

I. INTRODUCTION

There has been an increasing technological interest in cubic boron nitride (c-BN).¹⁻³ Among the super hard materials, c-BN has particularly fascinating properties, such as high thermal stability, low chemical reactivity, especially with ferrous materials, and an ability to be doped both n or p type. It can thus compete with diamond in many potential applications.²⁻⁴ Like diamond, c-BN is an sp^3 bonded structure and exhibits a stacking sequence of AaBbCcAa... in the [111] direction. However, it is difficult to synthesise pure c-BN and most cases it either comes as a mixture of phases⁵ or crystallises as a variable composition compound with defects and stacking faults.⁶

Electron Energy Loss Spectroscopy (EELS) is a premier diagnostic technique, especially for sub micron particles, since the focussing of the electron probe allows measurements to be taken from extremely small samples. In particular, there is great interest in the Energy Loss Near Edge Structure (ELNES). It can yield information on the bonding, local electronic structure and nearest neighbour coordination of the excited atom.^{7,8} This so-called coordination fingerprint can be used for the identification and quantification of unknown phases in complex systems such as the borides, nitrides, carbides and so on.^{9,10} The ELNES spectra of a sample can be obtained with a parallel EELS system mounted on a Scanning Transmission Electron Microscope (STEM) equipped with field emission gun (FEG).¹¹ In our case the FEG has an energy resolution of about 0.3V. Such a system can be competitive with X-ray Absorption Spectroscopy (XAS), especially where only small samples are available, and for the lighter elements.

The ELNES is the result of the transition of tightly bound core electrons to the unoccupied conduction band states induced by the passing of a swift electron. Hence ELNES probes the local density of unoccupied electronic states. Calculations of ELNES using self-consistent band theory methods^{12,13} and multiple scattering theory¹⁴⁻¹⁶ show reasonable overall agreement with available experimental spectra. Specifically, the ELNES of c-BN has been presented by many authors, both theoretically^{12,15,16} and experimentally.^{17,18} However, the detailed agreement between the experimental and calculated c-BN ELNES spectra has not been perfectly satisfactory. Either the resolution of the experimental spectra has been insufficient to reveal all the fine structure features produced in the theoretical calculations or the theoretical spectra have not fully reproduced the experimental fine structure. Although the correct number of observed peaks may be given by theory, their relative positions and intensities are often not correctly predicted. In this paper we present a comparison between state-of-the-art experimental (see Section II) and calculated (see Section III) c-BN ELNES. Not only do the new experimental results reveal practically all of the fine features found in the calculations, the positions and intensities of these features agree up to 60eV above the threshold.

II. EXPERIMENT

The c-BN powder used in these studies was produced and supplied to us by de Beers. These microcrystallites, a few microns in size and white in colour, were grown by a high-pressure and high-temperature route using hexagonal boron nitride (h-BN) as the starting material.

The specimens were prepared for the STEM measurements by grinding some of the powder using an agate pestle and mortar and then mixing it with a few drops of water. The tiny particles dispersed in the water were then collected onto a holey carbon film. The specimen was baked for a few hours in the microscope or exposed to the electron beam for some time to eliminate or reduce any carbon or other contamination. The EELS measurements were carried out in a Cambridge VG HB501 dedicated STEM fitted with an improved Parallel Electron Energy Loss Spectroscopy (PEELS) system by McMullan.¹¹ The HB501 is equipped with cold field emission gun operating at 100KV and has an energy spread of about 0.25eV. At present, our PEELS system gives a spectral resolution of about 0.35eV, as given by the full width at the half maximum of the zero-loss peak. Absolute energy measurements can be obtained to an accuracy of $\pm 0.3\text{eV}$, as judged by the π^* peak energy of C K-edge in graphite. We find it to be $285.37 \pm 0.3\text{eV}$, compared to a reported absolute energy value¹⁹ of $285.38 \pm 0.05\text{eV}$. Sufficiently thin regions of a c-BN flake suspended on a hole in the carbon support film were selected for recording spectra. All the spectra were acquired under the same conditions of a beam convergence semiangle of 13.2 mrad, and an effective spectrometer collection semiangle of 13 mrad. Under these conditions, to a good approximation, non-dipole transitions are not allowed because, for light elements, the inelastic scattering is strongly forward peaked.²⁰ For the ELNES region, spectra were acquired with an energy dispersion of 0.23eV/channel, in order to include the full range of the ELNES in one spectral region. Also, energy dispersions of 0.1eV/channel and 0.8eV/channel were used to acquire the spectra, to analyse the band gap region and the stoichiometry (B/N) respectively in the same region of the BN particle. In each case, a minimum of 10 spectra with a high number of counts each were acquired using long exposure times.

The processing of the spectra was accomplished using PEELS software developed in house. First, the dark-current was subtracted from all the spectra and flat fielded for a channel-to-channel gain correction. Second, each set of spectra (a minimum of 10) was aligned using a least square fitting algorithm and summed. From the resulting high loss region of the spectra the background was subtracted using the power law form, AE^{-r} . Then, to remove the effects of multiple scattering, the spectra were deconvolved by the raw low loss spectra (a Fourier-ratio deconvolution).⁷ Finally, each resulting spectrum was deconvolved by the zero-loss spectrum to remove the point-spread function.

III. CALCULATION

The electron energy loss function, for high-energy losses, is directly proportional to the imaginary part of the dielectric function, $\varepsilon_2(\mathbf{q}, E)$. Hence, within the single particle approximation, the measured intensity distribution of ELNES on the K-edge for a periodic system is given by:

$$\varepsilon_2(\mathbf{q}, E) = \frac{2\pi e^2}{\Omega \varepsilon_0 q^2} \sum_{\mathbf{k}, \text{c.b.}} |\langle \psi_{\mathbf{k}}^{\text{c.b.}} | e^{i\mathbf{q}\cdot\mathbf{r}} | \psi_{1s} \rangle|^2 \delta(E_{\mathbf{k}}^{\text{c.b.}} - E_{1s} - E) \quad (1)$$

where Ω is the unit cell volume, \mathbf{q} is the momentum transfer and \mathbf{k} is the k-point within the first Brillouin zone of the final state in the conduction band ($\langle \psi_{\mathbf{k}}^{\text{c.b.}} |$). The K-edge is given by the excitation from a 1s core state ($|\psi_{1s}\rangle$), so this is the initial state in the above

expression. The energies E_{1s} and $E_{\mathbf{k}}^{\text{c.b.}}$ denote the energy levels of the initial and final states respectively.

For the calculation of ELNES, the two main tasks are the evaluation of the density of unoccupied electronic states (DOS) term and the weighting transition matrix elements. In our scheme (which is described in detail by Pickard²¹ and elsewhere^{22,23}) the final states and energies $|\psi_{\mathbf{k}}^{\text{c.b.}}\rangle$ and $E_{\mathbf{k}}^{\text{c.b.}}$ are evaluated within an *ab initio* electronic structure calculation; using a total energy code (CASTEP) based on Density Functional Theory (DFT) within the Local Density Approximation (LDA). A plane wave basis set, periodic boundary conditions and non-local pseudopotentials are used.²⁴ Hence, the summation over all final states is the sum over all \mathbf{k} within the first Brillouin zone and all unoccupied bands c.b. at each k-point. An efficient Brillouin zone integration scheme has been adopted, which uses a very low k-point sampling and is based on an extrapolative approach.²⁵ The information for the extrapolation is obtained using $\mathbf{k}\cdot\mathbf{p}$ perturbation theory to second order within a set of sub volumes into which the Brillouin zone is divided. Some corrections to the $\mathbf{k}\cdot\mathbf{p}$ expansion are made for the use of non-local pseudopotentials²⁶. The resulting piecewise quadratic representation of the band structure is directly converted into a DOS using the analytic quadratic approach of Methfessel.²⁷

The representation of the wavefunctions in terms of plane waves allows the direct quantitative evaluation of the matrix element, in contrast to the more frequent approaches which are simply symmetry projected local DOS. In our evaluation of the matrix elements, the initial core states are taken from all electron calculations for the isolated atoms. In practice, the dipole approximation is applied. The directly evaluated matrix elements are then corrected for the pseudopotential error using the Projector Augmented Wave approach of van de Walle and Blochl.²⁸ Matrix elements evaluated in this way allow the absolute prediction of the cross-section with the correct dipole selection rules.

In order to compare our calculations with measured ELNES, particularly in insulators, it is important to consider the effects of the excitation process, in particular single particle core hole effects. These derive from the un-screening of the nuclear charge as an electron is excited from a localised core-state. In contrast to the situation in metals, in insulators the effect due to the core hole can be dominant, as the re-screening of the hole by the valence electrons is not complete. In our approach, the effects of the interaction between the core-hole and the ejected electron are treated by band structure methods but the remaining many body effects, which would lead to multiplet structure, are ignored.

In our current scheme, the effects of the core-hole on the unoccupied electronic states for systems with moderate core hole effects (eg. BN, diamond) are explicitly calculated by performing a supercell calculation in which there is a single excited potential in each cell. The supercell must be large enough that the neighbouring excited potentials do not interact with each other. For the c-BN system, the calculations are performed in a supercell comprising 2^3 primitive lattice cells. Then the spectra are evaluated for the excited atom. To model the excited atom, the more usual Z+1 approximation which would substitute, say, B by C, is improved upon by generating a special pseudopotential for the excited B atom with only one 1s electron.

IV. RESULTS AND DISCUSSION

The quality of the c-BN sample was assessed by X-ray powder diffraction (XRD) and EELS. The XRD pattern of the c-BN powders shows non-distorted peaks with relative intensity and d spacings very close to the reported c-BN standard XRD values (JCPDS 35-1365). The lattice parameter deduced by XRD is 3.616 ± 0.002 (the reported standard values are $a = 3.615$ or 3.620 ± 0.001). The EELS study of the composition and the stoichiometry of the particles confirm that the crystals used in our experiments are stoichiometric and free from contamination. The ELNES given in Figure 1 is from a defect free region of a c-BN particle about one mean free path thick which gives stoichiometry $B/N=1 \pm 0.03$. The bulk plasmon peak is measured to be 32.4 ± 0.2 eV.

Figure 1 shows the comparison between the experimental and calculated ELNES of the B and N K-edges of c-BN. The figure shows theoretical calculations with core-hole (thin solid lines) and without core-hole effects (dotted lines). Each calculated K edge is aligned to the energy of the peak labelled B and D for B and N K-edges respectively and the intensity is normalised to the height of peak B of the experimental spectra. While the calculated spectra is aligned with the experimental spectra as described, the energy scale is not adjusted. In the experimental ELNES, the features present show a breadth of 4eV or more, much greater than the experimental resolution.

At first glance, one can recognise the excellent agreement between the experimental and theoretical ELNES of both B and N K-edges. Both the peak positions and the relative intensities seen in the experimental results are reproduced by the calculations. A tabulation of the energies of the features in the experimental and calculated ELNES is given in Table I. The calculated spectra are convolved with a Gaussian whose width is 0.5eV which we believe to be comparable to the spectral resolution. However, lifetime broadening effects have been excluded from our theoretical calculations.

As can be seen by the comparison between the solid and dotted lines in Figure 1, core-hole effects dominate both the B and N K-edge ELNES at the threshold. By including core-hole effects, ELNES features up to 15eV above the edge onset are modified, giving close agreement to the experimental ELNES. Peaks A and B are particularly strongly modified by core hole effects. In the calculated ELNES, peak A at the edge onset has been enhanced over the experimental features for both the B and N K-edges. This may be due to an over estimation of the strength of the core hole. Up to 30eV above the threshold, the experimental ELNES features of both the B and N K-edges of c-BN are very similar to the equivalent XANES results of Chaiken *et al.*²⁹ Indeed, the absolute energy values are in close agreement with the XANES values (B K-edge: 194.5, 198.0 eV and N K-edge: 406.0, 409.0, 411.0 eV for peaks A,B,... respectively) given by Jimenez *et al.*³⁰ Peak A of the B K-edge is sharper and shifted to the lower energy in XANES, by comparison to that in the ELNES measurement. As described by Batson,³¹ this may be due to a reduction of the excitonic distortion by the incident swift electron in ELNES. Furthermore, this theoretical scheme correctly represents the EXELFS features, (G, H, I) up to 60eV above the edge, while at the same time, the peaks dominated by core-hole effects (up to 15eV from the threshold) are adequately enhanced. This is a feature particular to the plane wave approach, in that the upper and lower regions of the spectra are equally well represented by the basis set.

In summary, our experimental and theoretical ELNES show excellent agreement provided

that core-hole effects are included. However, we expect that further improvements will be made at higher energies by including lifetime broadening effects,³² and at the threshold by reducing the strength of the core-hole interaction.

ACKNOWLEDGEMENT

DNJ would like to thank the de Beers Industrial Diamond Division for the specimen and financial support. She would also like to thank New Hall College and The Cambridge Commonwealth Trust. CJP acknowledges the support of an EPSRC research studentship.

REFERENCES

- ¹ in *Synthesis and properties of boron nitride*, edited by J. Pouch and S. Alterovitz (Trans-Tech, Switzerland, 1990).
- ² J. Edgar, *J. Mater. Res.* **7**, 235 (1992).
- ³ L. Vel, G. Demazeau, and J. Etourneau, *Mater. Sci. Eng. B, Solid State Mater. Ad.Technol.* **10**, 149 (1991).
- ⁴ O. Mishima, in *Synthesis and properties of boron nitride*, edited by J. Pouch and S. Alterovitz (Trans-Tech, Switzerland, 1990), pp. 313–328.
- ⁵ D. McKenzie *et al.*, *J. Appl. Phys.* **70**, 3007 (1991).
- ⁶ N. Bezhenar, *Journal of super hard materials* **20**, 11 (1998), and references therein.
- ⁷ R. Egerton, *Electron Energy Loss Spectroscopy in the Electron Microscope* (Plenum, New York, 1996).
- ⁸ P. Rez, in *Transmission Electron Energy Loss Spectroscopy in Materials Science, EMPMD Monograph Series*, edited by M. Disko, C. Ahn, and B. Fultz (The Minerals, Metals & Materials Society, Warrendale, Pennsylvania, 1992), Chap. 5, p. 110.
- ⁹ R. Brydson, H. Sauer, and W. Engel, in *Transmission Electron Energy Loss Spectroscopy in Materials Science, EMPMD Monograph Series*, edited by M. Disko, C. Ahn, and B. Fultz (The Minerals, Metals & Materials Society, Warrendale, Pennsylvania, 1992).
- ¹⁰ F. Hofer and P. Golob, *Ultramicroscopy* **21**, 379 (1987).
- ¹¹ D. McMullan, P. Fallon, Y. Ito, and A. McGibbon, in *Electron Microscopy (EUREM) 92*, edited by A. R. *et al* (Universidad de Granada, Granada, Spain, 1992), Vol. 1, pp. 103–104.
- ¹² P. Rez, X. Weng, and H. Ma, *Micros. Microanal. Microstruct.* **2**, 143 (1991).
- ¹³ S. Kostlmeier, C. Elsasser, and B. Mayer, *Ultramicroscopy* **80**, 145 (1999).
- ¹⁴ J. Rehr, R. Albers, and S. Zabinsky, *Phys. Rev. Lett.* **69**, 3397 (1992).
- ¹⁵ A. Merchant, D. McCulloch, and R. Brydson, *Diamond and Related Materials* **7**, 1303 (1998).
- ¹⁶ M. Wubbelt, H. Kohl, and P. Kohler-Redlich, *Phys. Rev. B* **59**, 11739 (1999).
- ¹⁷ H. Schmid, *Micros. Microanal. Microstruct.* **6**, 99 (1995).
- ¹⁸ M. Jaouen *et al.*, *Micros. Microanal. Microstruct.* **6**, 127 (1995).
- ¹⁹ P. Batson, *Phys. Rev. B* **48**, 2608 (1993).
- ²⁰ R. Leapman, L. Grunes, P. Fejes, and J. Silcox, in *EXAFS Spectroscopy*, edited by B. Teo and D. Joy (Plenum, New York, 1981), p. 217.
- ²¹ C. Pickard, Ph.D. thesis, Cambridge University, Cavendish Laboratory, 1997.
- ²² C. Pickard and M. Payne, *Inst. Phys. Conf. Ser* **153**, 179 (1997).
- ²³ P. Rez, J. R. Alvarez, and C. Pickard, *Ultramicroscopy* **78**, 175 (1999).
- ²⁴ M. Payne *et al.*, *Reviews of Modern Physics* **64**, 1045 (1992).
- ²⁵ C. Pickard and M. Payne, *Physical Review B* **59**, 4685 (1999).
- ²⁶ C. Pickard and M. Payne, *Physical Review B* **62**, 4383 (2000).
- ²⁷ M. Methfessel, M. Boon, and F. Mueller, *J. Phys. C: Solid State Phys.* **16**, 1949 (1983).
- ²⁸ C. V. de Walle and P. Blöchl, *Physical Review B* **47**, 4244 (1993).
- ²⁹ A. Chaiken *et al.*, *Appl. Phys. Lett.* **63**, 2112 (1993).
- ³⁰ I. Jimenez *et al.*, *Phys. Rev. B* **55**, 12025 (1997).
- ³¹ P. Batson and J. Bruley, *Phys. Rev. Lett.* **67**, 350 (1991).
- ³² M. Kostner, Master's thesis, Vienna University of Technology, 2001.

TABLE I. Comparison of the energies of the features in the experimental and calculated ELNES for the boron and nitrogen K-edges. The asterix (*) denotes the alignment peak in each case.

Boron	A	B*	C	D	E	F	G	H	
Exp.	195.5	198.1	201.0	205.3	207.2	210.6	215.2	224.0	
Calc.	196.2	198.1	200.3	204.4	207.0	209.9	215.4	224.2	
Nitrogen	A	B	C	D*	E	F	G	H	I
Exp.	406.4	409.4	411.5	416.4	423.7	431.2	437.5		
Calc.	406.7	408.4	411.6	416.4	423.3	431.5	437.9	450.8	455.7

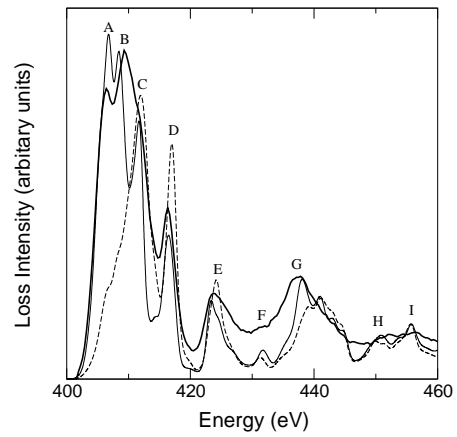
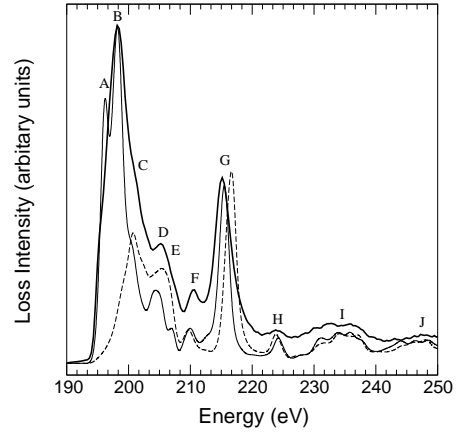


FIG. 1. Experimental ELNES (thick solid lines), theoretically calculated ELNES with core-hole effects (thin solid lines), and theoretically calculated ELNES without core-hole effects (thin dotted lines) of the boron K-edge (top) and the nitrogen K-edge (bottom) in cubic boron nitride.